Code Development for Calculating Electron Beams in the Cavities of the Future High-Power Gyrotrons*)

Tomoharu NUMAKURA, Tsuyoshi KARIYA, Ryutaro MINAMI, Maki OKADA, Toshitaka HOJO, Fumiya MOTOYOSHI and Tsuyoshi IMAI

Plasma Research Center, University of Tsukuba, Tsukuba 305-8577, Japan

(Received 16 September 2018 / Accepted 4 February 2019)

This study develops a computational code for evaluating the operations of high-power gyrotrons with high-current electron beams. The analytical model describes the electromagnetic fields and electrons by the Maxwell equations and cold-fluid equations, respectively. Specifically, it estimates the output power of the gyrotron with electron-beam fluctuations, which occur under high beam currents. The effects of fluctuations of the intense electron flows in nonuniform magnetic fields are studied in a 1 MW gyrotron for electron cyclotron resonance plasma heating and current drive in large devices, such as the tandem mirror plasma device GAMMA10/PDX and the Large Helical Device (LHD). The rate of fluctuation growth of the electron beam and the output power of the high-power gyrotron with a fluctuated beam are calculated. In gyrotrons with a higher operating frequency (e.g., 154 GHz), significant deterioration of the electron beam and gyrotron operation is expected at beam currents exceeding 120 A.

Keywords: gyrotron, computational code, high current, beam fluctuation, output power

DOI: 10.1585/pfr.14.2405052

1. Introduction

High-power millimeter-wave gyrotrons are designed for continuous-wave or long-pulse operation in fusion plasma applications. Gyrotrons are attractive sources of high-power millimeter and submillimeter waves for electron cyclotron heating and current control of magnetically confined plasmas in controlled fusion research. For these purposes, the gyrotrons must operate in the quasi-continuous regime at frequencies of 10 - 300 GHz and output powers of 1 MW or higher. Recently, many studies [1–3] have been devoted to high-power and long-pulse gyrotrons, and multi-frequency gyrotrons are required for experimental flexibility and research collaboration efforts.

Two important requirements of gyrotron development are high radiated power and stable operation in the single desired mode. The efficiency and limitations of the attainable gyrotron parameters are determined by the quality of the electron beam formed in the gyrotron. High-power gyrotrons require a high-current electron beam with a sufficiently small velocity spread and a transverse structure. The efficiency and output power of a gyrotron are significantly restricted by the spread in both the transverse velocity and the beam structure. For future gyrotron development, this study develops a computing code that describes the interaction of the electron beam with the width in waveguide-cavity gyrotron oscillators. Several studies [4–7] have confirmed that fluctuations of the electron beam influence nonuniform magnetic fields and crossed fields. Theoretically and experimentally, a low-quality beam is known to induce various parasitic instabilities that evolve in gyrotron operations. By studying these fluctuations, we can understand various phenomena that affect the beam quality.

The developed code calculates the profile of the electron beam by simultaneously solving a set of cold-fluid equations of motion and the Maxwell equations. The code reaches a self-consistent solution in the dynamic system that accounts for the effects of electron-beam fluctuations. A parallel algorithm [8, 9] ensures the required calculation accuracy and reduces the computation time. We present the calculation results for a 1 MW gyrotron.

2. Fluctuation Model for Electron Beams

In the analytical model, we consider the open resonator of a gyrotron formed by a section of a cylindrical hollow waveguide. The radius of the waveguide varies slightly along its axis. As the waveguide possesses cylindrical symmetry, it was modeled in cylindrical polar coordinates (r, θ, z). The applied magnetic field was directed along the z-axis, perpendicular to the cross-section. The electron density of the annular beam was piecewise defined as a function of the radius r. The radial electron distribution $n_e(r)$ was limited to the region $r_e - r_b < r < r_e + r_b$, where r_e is the radius of the center of the beam and r_b is

author's e-mail: numakura@prc.tsukuba.ac.jp

*) This article is based on the presentation at the 12th International Conference on Open Magnetic Systems for Plasma Confinement (OS2018).

the beam width. Therefore, the density was calculated as

$$n_e(r) = H(r - r_e + r_b)H(r_e + r_b - r)n_0/8\pi r_e r_b, \quad (1)$$

where H is the step function and the coefficient n_0 was calculated from the beam current I and the electron velocity V. The current I is given by

$$I = n_e V = n_0 V/8\pi r_e r_b. \quad (2)$$

The fluctuation will prevent a sharply localized electron beam [4].

Before investigating the effect of beam fluctuations, we must determine the stationary state of the system. The electromagnetic field components E and B accompanying the electron beam in the stationary state are respectively given by

$$E_0 = E_{0r}(r) \quad \text{and} \quad B_0 = B_{0z}(r) + B_{0\theta}(r). \quad (3)$$

The velocities of the electron beam in the fluid description is

$$V_0 = V_{0z}(r) + V_{0\theta}(r). \quad (4)$$

In the cold-fluid model, the average r-component of the velocity is zero. The stationary state is determined from the Maxwell equations and the cold relativistic fluid Euler equations [4]. Here the subscript 0 denotes the stationary value of a quantity. As mentioned in [4], the axial magnetic field B_{0z} is constant in regions of zero electron density, and the magnetic fields along the axis and the wall are very similar, reflecting the small contribution from the electron current. The nonuniformity is considered to occur in regions of non-zero density of the beam current.

In the framework of small-perturbation theory [4], the quantities in the equations are superpositions of stationary values and small time- and θ-dependent fluctuations: $E = E_0 + \delta E$, $B = B_0 + \delta B$, $V = V_0 + \delta V$ and $r_b = r_{b0} + \delta r_b$. As the fluctuations are small, the equations can be linearized and written to first order in the fluctuated quantities. The time dependence of the azimuthal angle θ is $\exp(i(\lambda\theta - \omega t))$, where ω and t are the frequency and time, respectively, and λ is the order. If ω is complex with $\mathrm{Im}(\omega) > 0$, then the fluctuation will grow exponentially as $\exp(\mathrm{Im}(\omega))$. Under the symmetric conditions of the gyrotron, the azimuthal electrical field on the axis must vanish, i.e., $\delta E_\theta = 0$ at $r = 0$. Therefore, $\lambda = 1$ is forbidden and the minimum λ is $\lambda = 2$. The boundary conditions in a hollow waveguide are $\delta E_0(r = r_w) = 0$, where r_w is the radius of the waveguide.

Following Ref. [4], the dispersion relation D of the frequency ω is derived from the boundary condition as follows:

$$D(\omega) = AJ'_\lambda(\omega r_w) + CY'_\lambda(\omega r_w) = 0, \quad (5)$$

where the functions J'_λ and Y'_λ are the derivatives of the Bessel function and the Neumann function of integer order λ, respectively. The coefficients A and C that depend on the parameters ω and λ are calculated by:

$$\delta E_\theta(r_e + r_b) = AJ'_\lambda(\omega(r_e + r_b)) + CY'_\lambda(\omega(r_e + r_b)). \quad (6)$$

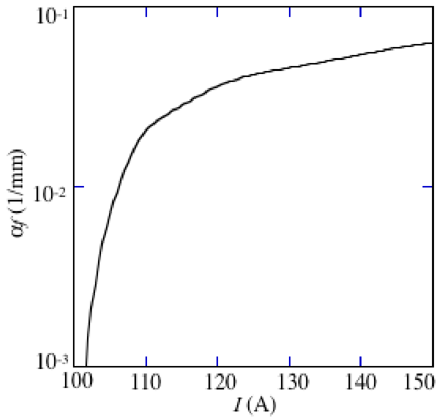

Fig. 1 Fluctuation factor α_f as a function of the beam current I at $r_w = 20$ mm.

We must now find the zero points of the dispersion relation, $D(\omega) = 0$. The most efficient approach is to solve the dispersion relation Eq. (5) while simultaneously varying $\mathrm{Re}(\omega)$ and $\mathrm{Im}(\omega)$ until D is minimized. To minimize the D, we adopted a numerical method of simulated annealing [8]. A modification of the downhill simplex method, this method determines D as a function of the best point of $\mathrm{Re}(\omega)$ and $\mathrm{Im}(\omega)$ from the starting simplex. This heuristic optimization of D is calculated by a parallel algorithm that utilizes the added computational power of the parallel architecture to enhance the optimization performance (i.e., the convergence rate) of the algorithm. The execution time is reduced by parallel calculations of the simplex operations, such as recalculating the D values.

The beam travels in the z-direction at velocity V_{0z} with a fluctuation that increments by $\mathrm{Im}(\omega)$. The ratio α_f, defined as the ratio of the growth rate of the fluctuation $\mathrm{Im}(\omega)$ and the average axial velocity, is given by

$$\alpha_f = V_{0z}/\mathrm{Im}\omega. \quad (7)$$

The factor α_f corresponds to the distance traveled by the electron beam when the amplitude of the fluctuation has grown by the factor e. Figure 1 plots α_f as a function of the beam current I at $r_w = 20$ mm. Here we show the result of $\lambda = 2$ (the α_fs for $\lambda > 2$ are negligible in the 28-GHz and 154-GHz gyrotrons, as mentioned in Sec. 4). The factor α_f increased with increasing beam current and applied magnetic field, and rapidly decreased with increasing λ. We calculated the fluctuation level from the $\mathrm{Im}(\omega)$ value and the electron-beam parameters (including the deviation of the beam width outside of the electron gun, which is obtained by the electron trajectory code) [10]. For a gyrotron operating at $I = 100$ A, $r_w = 20$ mm and $B_0 = 6.2$ T through the midsection of the cavity, the factor

α_f is 0.00024. If the cavity is located more than 100 mm from the electron gun and the current is below 120 A, the fluctuation exerts no significant effect on the quality of the electron beam.

3. Interaction Model for Radio Frequency (RF) Fields

We first investigated the electron interaction with RF waves in a gyrotron with a fluctuating electron beam. The RF field $\boldsymbol{E}$ in the cavity is expressed as a superposition of transverse electric (TE) cavity modes in cylindrical coordinates (r, θ, z):

$$\boldsymbol{E} = \Sigma_{mn} V_{mn} \boldsymbol{e}_{mn} \exp(i\omega_{mn} t), \tag{8}$$

where V_{nm} is the field amplitude and ω_{nm} is the frequency of the mode. The function $\boldsymbol{e}_{nm}$ characterizes the eigenvector of the corresponding TE mode with indices m and n, and is determined by the Helmholtz equation:

$$\Delta_\perp \boldsymbol{E} + k_{mn}^2 \boldsymbol{E} = 0, \tag{9}$$

where the complex transverse wave number k_{nm} is determined by the boundary condition of the cavity. Considering Eqs. (8) and (9) and the condition of the stable state, the complex function V_{nm} obeys the following parabolic equation:

$$\partial^2 V_{mn}/\partial z^2 + [\omega_{mn}^2/c^2 - k_{mn}^2 + I_c]V_{mn} = -4\pi/c^2\, \partial I/\partial t. \tag{10}$$

Equation (10) describes the temporal evolution of the field amplitude along the axis of the cavity under interaction with the electron beam. I_c is the small correction term in Ref. [11]. The total current term I is given by integrating the cross-section of the product of the function $\boldsymbol{e}_{nm}$ and the electron density n_e related to the electron beam [2]:

$$I = 2\pi e \int n_e(r) \boldsymbol{V} \cdot \boldsymbol{e}_{mn} r dr. \tag{11}$$

If the electron density distribution is assumed as the delta function $\delta(r - r_e)$, then the coupling of the electrons in the beam with radial coordinate r to the rotating TE_{mn}-waves derived from Eq. (11) can be described by the following function (see e.g., Ref. [2]):

$$L_s = J_{m-s}(k_{mn} r_e). \tag{12}$$

In Eq. (12), s is the cyclotron resonance harmonic number. In this case, the electron-beam radius r_e is chosen to maximize the absolute value of L_s [2]. As the electron beam has a width, we can derive from Eq. (11) the coupling parameter of the electron beam to the RF field in a gyrotron with a piecewise-constant beam:

$$L_s = \int J_{m-s}(k_{mn} r) r dr / 4 r_b r_e. \tag{13}$$

Figure 2 plots the dependence of the coupling parameter L_1 on the beam width r_b for a gyrotron operating in

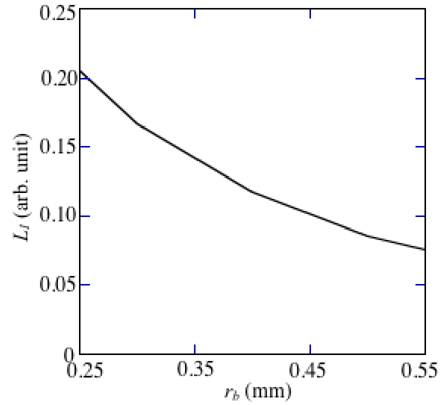

Fig. 2 Coupling parameter L_1 as a function of the width of the beam distribution r_b.

$TE_{28,9}$ mode at $r_e = 9.1$ mm and $r_w = 20$ mm. Assuming a delta-function profile of the beam and using Eq. (12), L_1 was calculated as 0.217, higher than all values of L_1 in Fig. 2 (which assumed a piecewise-constant function of the beam profile). The coupling parameter L_1 decreased with increasing width r_b, meaning that the fluctuations in the electron beam reduced the gyrotron efficiency.

4. Effect of the Beam Fluctuation on the Output

This section numerically investigates the electron-beam fluctuation in a 1 MW gyrotron with a cylindrical hollow cavity, the current design of large devices such as the LHD. The cavity operates at 154 GHz in $TE_{28,9}$ mode, and the gyrotron operates at the fundamental cyclotron resonance.

The calculation parameters were set to the typical gyrotron operating parameters (electron-beam voltage and current of 80 kV and 60 A respectively from the electron gun, with a measured output power of 1.25 MW). The corresponding pitch factor α was 1.1. The geometry of the cavity and the magnetic field profile are shown in Fig. 3 (a). Figure 3 (b) shows the typical RF field profile of the operating mode gyrotron at 154 GHz and the average Lorentz factor γ related to the kinetic energy of the electrons in the absence of beam fluctuation effects. The current of the electron beam was $I_0 = 60$ A and the calculated output power was 1.47 MW. The transmission efficiency from the mode convertor to the window was ignored in this calculation.

Figure 4 (a) plots the calculated pitch factor fluctuation $\delta\alpha$ and width of the electron beam in the gyrotron as functions of beam current when the beam passed through the midsection of the cavity. The beam parameters (including the fluctuation levels outside the electron gun of the gyrotron) were obtained by EGUN code [10]. The $\delta\alpha$ was obtained from the perpendicular velocity fluctuations.

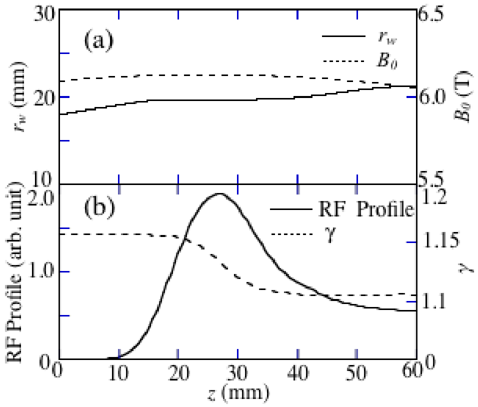

Fig. 3 Dependence of the cavity radius r_w (solid curve), applied magnetic field strength B_0 (dashed curve) in (a), RF profile (solid curve), and the average Lorentz factor γ of the electrons (dashed curve) in (b) as a function of the axial position z in the cavity for the $TE_{28,9}$ mode at 154 GHz.

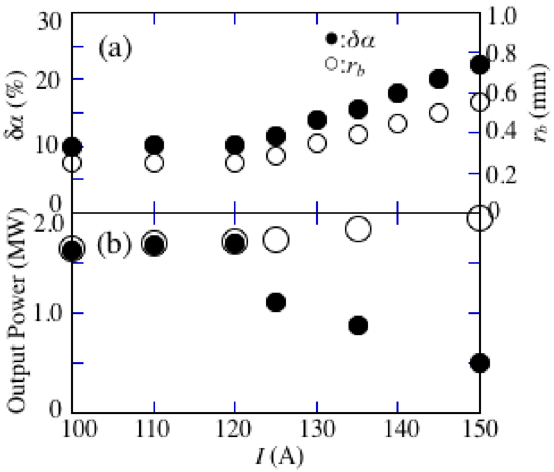

Fig. 4 Dependence of the fluctuation of the pitch factor $\delta\alpha$ (filled circles), the width of the electron beam r_b (open circles) in (a), the output power of the gyrotron without (open circles) and with the fluctuation (filled circles) as a function of the beam current I.

Both $\delta\alpha$ and r_b increased when the beam current exceeded 120 A. Figure 4 (b) shows the beam-current dependence of the gyrotron output power. Increasing either of $\delta\alpha$ or r_b decreased the gyrotron output power. These results indicate that at high beam current ($>$ 120 A), the fluctuations significantly deteriorate the quality of the electron beam. However, the degradation of the output power in the 1 MW gyrotron developed for the GAMMA10/PDX tandem mirror [12] (80 kV, operating in $TE_{8,5}$ mode at 28 GHz [9]) was not calculated, because the growth rates of the large current fluctuations in the cavity were negligible at low RF-operating frequency under a small applied magnetic field. The fluctuation becomes significant in a certain region of the parameter space. This result will be important in future gyrotrons with higher operating frequency (such as 154 GHz) and output power, which will require a high beam current.

We will continue our attempts to develop gyrotrons that can operate over a wide frequency range (14 - 300 GHz) for present and future devices up to Demonstration Power Station (DEMO), the next-generation nuclear fusion power plant [3, 13, 14].

Acknowledgments

This work was partially supported by the grant-in-aid for scientific research from the Ministry of Education, Science, Sports and Culture of Japan (26249141).

[1] G.S. Nusinovich, *Introduction to the Physics of Gyrotrons* (Johns Hopkins University Press, 2004).
[2] M.V. Kartikeyan *et al.*, *Gyrotrons* (Springer, Berlin, 2003).
[3] T. Kariya *et al.*, Nucl. Fusion **57**, 066001 (2017).
[4] R. Schuldt and E. Borie, Int. J. Infrared Millim. Waves **16**, 1675 (1995).
[5] O.I. Louksha *et al.*, Tech. Phys. **58**, 751 (2013).
[6] O. Dumbrajs and G.S. Nusinovich, Phys. Plasmas **20**, 073105 (2013).
[7] R. Yan *et al.*, Phys. Plasmas **15**, 103102 (2008).
[8] T. Numakura *et al.*, Trans. Fusion Sci. Technol. **63**, 295 (2013).
[9] T. Numakura *et al.*, AIP Conf. Proc. **1771**, 030023 (2016).
[10] W.B. Herrmannsfeldt, SLAC-331-UC28, Stanford Linear Accelerator Center (1988).
[11] A.R. Choudhury *et al.*, IEEE Trans. Electron Devices **62**, 192 (2015).
[12] Y. Nakashima *et al.*, Nucl. Fusion **57**, 116033 (2017).
[13] T. Kariya *et al.*, Int. J. Infrared Millim. Waves **32**, 295 (2011).
[14] T. Imai *et al.*, J. Plasma Fusion Res. **85**, 378 (2017).